Progress In Electromagnetics Research M, Vol. 24, 167–178, 2012

RADAR IDENTIFICATION OF HOSTILE FIRE BY MEANS OF THE ELECTROMAGNETIC COMPLEX NATURAL RESONANCES OF PROJECTILES

S. W. Harmer*, S. E. Cole, and N. J. Bowring

Sensing and Imaging Group, Manchester Metropolitan University, England

Abstract—The authors discuss and demonstrate the feasibility of using ultra wide band microwave radar to detect and identify small arms fire. Detection and tracking is by standard radar techniques, but identification is carried out by exciting the projectiles Complex Natural Resonances and using this aspect independent information to assign a caliber to the incoming projectiles. The typical sizes of small arms projectiles (calibers 5.56 mm through to 13 mm) imply that ultra wide band illumination in the microwave region of the spectrum between 1.5–5.5 GHz is required to excite these object's fundamental resonances. The authors give a discussion of the effects of motion on the quality of the complex natural resonance data obtainable and present both simulated and laboratory data for the radar cross section of three different caliber projectiles (5.56 mm, 7.62 mm and 13 mm).

1. INTRODUCTION

There is a current trend into the development of Hostile Fire Indication (HFI) systems which can detect, track and locate firing position of incident small arms fire. Such systems have widespread military application and possible homeland security application. Example military scenarios include protecting infantry troops from sniper fire by revealing firing location and protecting both land and airborne vehicles from incident fire. One possible homeland security scenario is where one needs to be able to rapidly locate a sniper who has fired at a target, for example to locate someone covertly firing on a campus grounds or at a large event. At the present time most proposed or commercially available systems are based on passive

Received 13 March 2012, Accepted 17 April 2012, Scheduled 21 April 2012

* Corresponding author: Stuart William Harmer (s.harmer@mmu.ac.uk).

acoustic technology or on infrared imaging. Radar HFI systems are still only in research and development phase. Radar HFI systems offer considerable advantages over their passive rivals, being able to detect and locate firing positions when acoustic muzzle blast and optical flash are absent or when the projectile is travelling at subsonic speeds. Additionally, with a radar approach, it is possible to utilize a well known electromagnetic phenomenon to give reliable information on the type and size of the projectile. Such capability is currently lacking from passive HFI systems. The caliber of the projectile is useful as it allows a better estimation of firing location when a partial projectile trajectory is measured. Larger, heavier caliber projectiles are decelerated less than smaller, lighter projectiles by air resistance. Consequently an estimation of the caliber, and therefore mass, of a projectile can assist in the accurate determination of firing location by inputting an extra piece of relevant information to a ballistic model. The caliber of projectiles is also useful in being able to assess enemy capability and may also help to mitigate 'friendly fire' incidents where friendly forces and enemy forces may use different caliber projectiles.

2. PROPOSED SOLUTION

It is well known that a highly conductive body possesses an infinite set of electromagnetic Complex Natural Resonances or CNR [1–6]; and that the fundamental resonance occurs when the wavelength of the exciting radiation is approximately twice the length of the object's longest linear dimension [3, 4]. The most commonly known example of this phenomenon is Mie scattering, which is the scattering of electromagnetic waves from a conducting sphere. In this case the Radar Cross Section (RCS) of the sphere presents oscillatory behavior with frequency as the incident electromagnetic waves constructively or destructively interfere around the sphere [7, 8].

Since an antenna only emits electromagnetic waves over a finite bandwidth, only excitation of a partial set of CNR is possible. The CNR allows the object's signature to be mapped, in two dimensional complex frequency space (i.e., the s-plane). Since the position of these CNRs in complex frequency space is dependent only upon the size and shape of the object's conducting surface, they further allow an aspect, or orientation, independent identification of the object to be made based solely on the position of its partial set of CNR [9, 10].

Application of this phenomenon to the Radar detection and recognition of airborne projectiles is useful, as the set of CNR can be employed to give very valuable information on the dimensions of the projectile whilst in flight — allowing the determination of

projectile caliber. Additionally, the RCS of the projectile can be significantly enhanced at the CNR frequencies and this important fact makes detection, ranging and tracking the incident projectiles more effective. Although this technique has been long applied to the Radar identification of much larger airborne objects, such as aircraft and missiles [11–15], the possibilities of detection and identification of much smaller objects has been largely overlooked.

It is proposed that CNR excitation of the incident projectiles within the transmitted radar beam can be achieved using frequency modulated pulses, such as a linear chirp. This ultra wideband (UWB) waveform will excite a useful subset of CNRs which are encoded within the scattered signal. The scattered signal is then detected at the receiving antennae array. Post reception signal processing, such as conventional matched filtering (i.e., replica correlation implemented as fast convolution), as is commonly employed within the processing of FM radars to enhance SNR can be extended to include some other analysis techniques which apply deconvolution algorithms to extract the CNR information of interest. Various dedicated signal processing and/or pattern recognition techniques may also be applied to extract and analyze these characteristic signal components in order to identify or classify the incident projectile.

3. THEORETICAL BASIS

The impulse response of the projectile is given by the well known equation, which was formalized by Baum in his treatise on the Singularity Expansion Method or SEM [1],

$$h(t) = \frac{1}{2}\sum_{m=1}^{M}\left(C_m \exp(Z_m t) + C_m^* \exp(Z_m^* t)\right) \tag{1}$$

In the frequency domain the impulse function is,

$$H(\omega) = \frac{1}{4\pi}\sum_{m=1}^{M}\left(\frac{C_m\left(Z_m^* - i\omega_m\right) + C_m^*\left(Z_m^- i\omega_m\right)}{\omega^2 - \omega_m^2 - \alpha_m^2 + i2\alpha_m\omega_m}\right) \tag{2}$$

where $Z_m = \alpha_m + i2\pi\nu_m$ are the aspect independent CNR frequencies of the object, and M is the number of CNR's excited. The complex amplitudes C_m depend upon the form of the illuminating pulse and the orientation of the target and therefore are not useful for target identification purposes, but are useful for ranging to target and in flight tracking using conventional radar methods. The model order M depends on the bandwidth of the microwave illumination, and the target's shape.

The projectile impulse response, convolved with the transmitted radar waveform, the impulse response of the transmitter and receiver antennae, constitutes the Late Time Response (LTR) of the system.

$$S = P \otimes T \otimes R \otimes h + N \tag{3}$$

Here $\otimes$ denotes the discrete one dimensional convolution operation, and P and h are the radar waveform before transmission and the target impulse response, respectively. T and R denote transmitter and the receiver impulse responses respectively, and N is the noise term.

The effect of projectile motion upon the impulse response, see Equation (1), is an important consideration for the intended application. Two effects of motion are possible: Doppler shift of the CNR frequencies and the alteration of aspect during the radar pulse duration. The first effect is very small; the maximum magnitude of the Doppler shift, $\Delta\nu = \frac{u}{c}\nu$ (where $u = 1000\,\mathrm{ms}^{-1}$ and ν is the incident frequency). The Doppler shift is less than 13 kHz for the fundamental CNR frequency of a 7.62 mm caliber projectile ($\nu = 3.52\,\mathrm{GHz}$, see Figure 1) travelling at $1000\,\mathrm{ms}^{-1}$ relative to the radar. The second effect can be more significant and, not being quite as obvious or widely known as the Doppler effect, requires a more detailed explanation. The CNR of projectiles are excited by the transmitted radar waveform, for example a linear chirped pulse, and during the pulse duration the projectile will move, and in general will alter aspect with respect

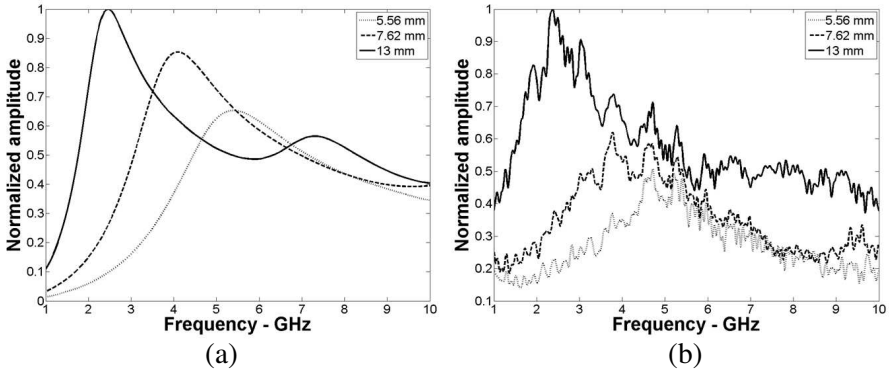

Figure 1. The CNR of three different caliber projectiles (5.56 mm, 7.62 mm and 13 mm) as (a) simulated in a finite time domain electromagnetic solver package and (b) obtained experimentally in an anechoic chamber in the laboratory. There is good agreement between prediction and experiment suggesting that the CNR approach will allow indentification and discrimiation of the caliber of incoming small arms fire.

to the radar. The alteration of aspect does not explicitly affect the CNR frequencies present (Z_m in Equation (1)) but does affect the amplitude of the CNR (C_m in Equation (1)). This effect can blur the position and width of the CNR and in extremis may prevent the accurate determination of projectile caliber. The extent of this motion induced blurring will depend on the time duration of the exciting radar waveform, the velocity of the projectile and the orientation of the object during the excitation phase.

Equation (1) is now written as

$$h(t) = \frac{1}{2}\sum_{m=1}^{M}\left(C_m\left(\underline{r}(t)\right)\exp\left(Z_m t\right) + C_m^*\left(\underline{r}(t)\right)\exp\left(Z_m^* t\right)\right) \quad (4)$$

We have now written the complex amplitudes C_m explicitly in terms of the time dependent position vector of the incoming projectile, $\underline{r}(t) = x(t)\,\underline{\hat{x}} + y(t)\,\underline{\hat{y}} + x(t)\,\underline{\hat{z}}$. Therefore, when the impulse response is convolved with transmitter and receiver impulse responses and with the radar pulse, as is done in Equation (3), the detected signal is modified by the fact that the complex amplitudes C_m now vary with position, and hence with time.

$$\begin{aligned} S(t) \;=\; & \frac{1}{2}\sum_{m=1}^{M} P(t) \otimes T(t) \otimes R(t) \\ & \otimes \left(C_m\left(\underline{r}(t)\right)\exp\left(Z_m t\right) + C_m^*\left(\underline{r}(t)\right)\exp\left(Z_m^* t\right)\right) + N(t) \end{aligned} \quad (5)$$

The C_m terms can be expanded as a Taylor series in time, where we assume that we will only require terms up to those linear in time to adequately describe the variation in the amplitude terms C_m over the time period of the pulse. This assumption is likely to be a very good one for incoming small arms projectiles as they have a speed which is $\leq 1000\,\mathrm{ms}^{-1}$; whereas a reasonable chirped radar pulse might last for a millisecond — giving a total displacement of ≤ 1 meter. At a range of 100 meters this displacement results in an angular change of less than 0.5 degrees, meaning that the alteration of aspect is likely to be very minor under such conditions.

Assuming, without loss of generality, that the radar pulse is incident upon the projectile at a time $t = 0$, and expanding the C_m terms as a Taylor series up to those terms linear in time, Equation (5) can be written approximately as,

$$S(t) \approx X(t) \otimes \left(h_0(t) + h_1(t)\right) + N(t) \quad (6)$$

where, $X(t) = P(t) \otimes T(t) \otimes R(t)$, and

$$h_0(t) = \frac{1}{2}\sum_{m=1}^{M}\left(C_m\left(\underline{r}(0)\right)\exp\left(Z_m t\right) + C_m^*\left(\underline{r}(0)\right)\exp\left(Z_m^* t\right)\right) \quad (7)$$

is the impulse response for a stationary object, and the contribution to the impulse response from the object's motion is given by,

$$h_1(t) = \frac{1}{2}\sum_{m=1}^{M}\left(D_m t \exp(Z_m t) + D_m^* t \exp(Z_m^* t)\right) \tag{8}$$

and

$$\begin{aligned} D_m &= \frac{\partial C_m(\underline{r}(0))}{\partial x}\frac{dx(0)}{dt} + \frac{\partial C_m(\underline{r}(0))}{\partial y}\frac{dy(0)}{dt} + \frac{\partial C_m(\underline{r}(0))}{\partial z}\frac{dz(0)}{dt} \\ &= \underline{\nabla} C_m(\underline{r}(0)) \cdot \frac{d\underline{r}(0)}{dt} \end{aligned} \tag{9}$$

where the symbol $\cdot$ is used to denote the scalar product.

Equation (6) suggests, perhaps unsurprisingly, that the effects of motion on the impulse response of the projectile can be considered as a linear perturbation to the stationary impulse function. The frequency domain representation of the part of the impulse function related to motion effects, i.e., $h_1(t)$, is given by the Fourier transform of Equation (8),

$$\begin{aligned} H_1(\omega) &= \frac{1}{4\pi}\sum_{m=1}^{M} D_m \frac{(1-\exp((Z_m - i\omega)\tau))(1-(Z_m - i\omega)\tau)}{(Z_m - i\omega)^2} \\ &\quad + \ldots D_m^* \frac{(1-\exp((Z_m^* - i\omega)\tau))(1-(Z_m^* - i\omega)\tau)}{(Z_m^* - i\omega)^2} \end{aligned} \tag{10}$$

Clearly, if the components of the velocity of the projectile are small and the change of complex amplitude with position is also small relative to the stationary amplitudes, then the effects of the motion of the projectile on the impulse function will be minimal. These conditions are only expected not to apply where the projectile is near to the radar system, and hence the aspect will alter significantly during illumination by a single pulse. Or where the projectile is traversing the radar beam, rather than heading radially toward the radar. However, provided the product of pulse duration and velocity of projectile is small, only projectiles passing very near to the radar system will have significant blurring of CNR due to motion effects.

4. INITIAL RESULTS

The experimental data presented in Figure 1 was taken with an Agilent E8363b PNA, connected with two 1–18 GHz Vivaldi horn antennae. The projectiles were mounted on an expanded polystyrene stand within an anechoic chamber and illuminated by stepping the

Figure 2. Photograph of the projectiles used for RCS measurement within an anechoic chamber, a quarter dollar coin is included for scale. The projectiles were made of steel and are representative of the shape and size of similar caliber military projectiles classed as small arms fire.

frequency between 1 GHz and 10 GHz in 801 discrete steps. The aspect of the projectile was adjusted so as to maximise the received signal, the optimum aspect was found to be with the projectile's axis of symmetry parallel to the direction of the electric field transmitted form the antenna, see figure Figure 3.

The projectiles (see Figure 2) were placed, stationary, one meter from the transmitter/receiver setup and the transmitted power was set at -17 dBm. Application of the well known radar equation, where received power $\propto \frac{P}{R^4}$ (where P is the transmitted power and R is the range), suggests that similar results could be obtained at a range of 15 meters with a 1 W pulsed transmit power or at a range of 85 metres with a 1 kW pulse power. Figure 1 shows that there is a clear similarity between the normalised RCS predicted in simulation and that obtained in our laboratory measurements. The raw frequency domain data from the UWB sweep was subject to deconvolution with the antenna response to attempt to remove the frequency response of the antenna and source. The experiemental data has then been smoothed by application of a low pass filter to remove some unwanted high frequency ripple that is probably caused by mismatch between antenna and source and by standing waves between antenna and target. The data presented in table one was obtained by application of the Generalized Pencil Of Functions (GPOF) method to the time domain signals. This technique is very succesful at decomposing signals that are of the form given by Equation (1) into their constituent resonances [10, 16]. Although there are two CNR predicted by simulation within the frequency sweep taken (1–10 GHz) for the 13 mm projectile, the second CNR is not well resolved experimentally (see Figure 1).

The Radar Cross Section presented by projectiles of different calibers is highly dependent upon the aspect of the projectile with respect to the radar and the polarization of the incident radar pulse with respect to the projectile orientation (see Figure 3). The RCS was calculated for a pulse that contains equal power density at all frequencies over the range 1.5–5.5 GHz, thus the RCS here represents a broadband RCS that is consistent with an expected return of a broad band pulse. In reality the RCS is dependent on the frequency of incident radiation and this dependence is oscillatory as the projectile is within the Mie scattering regime. In order to evaluate the possibility of detection of an object that presents such as small RCS (maximum 9 cm^2 in optimum configuration, see Figure 3) an example antenna consisting of a phased array of patch antenna is postulated for both the radar transmit and receive functions. The antenna will be sensitive to frequencies in the 1.5–5.5 GHz region of the microwave spectrum and consists of 1000 elements equally spaced 5 cm from each other in the array; the area of each element is assumed to be 4 cm^2. Such electrically small antenna will radiate in a near isotropic fashion; and the gain of each individual element is assumed to be 0 dB. This postualted phased array is just capable of radiating over the 4 GHz bandwidth without

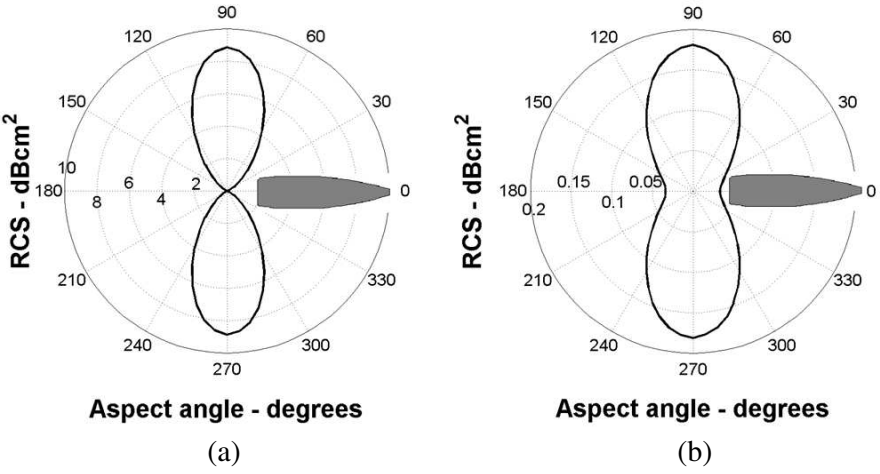

Figure 3. Graphical illustration of the simulated broadband (1.5–5.5 GHz) RCS in cm^2, as measured with a co-polarized receiver, for a 7.62 mm caliber projectile with aspect angle (0 degrees being along the length of the projectile). The upper plot is for the scenario where the polarization of the incident radar pulse has the electric field component parallel with the projectile axis; the lower plot is the case where the electric field is perpendicular to the projectile axis.

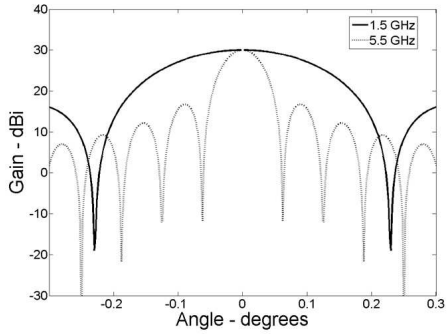

Figure 4. Examples of predicted beam patterns for the phased array outlined for detection of projectiles. The beams are shown for the highest (5.5 GHz) and lowest (1.5 GHz) frequencies transmitted.

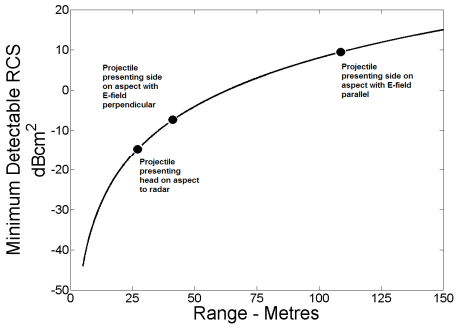

Figure 5. A graph showing the simulated minimum detectable RCS, for a SNR of 10 dB, versus range for the 1000 element phased array antenna discussed. The total power transmitted is 100 W, giving a radiated power of 100 mW per array element. The RCS of a 7.62 mm caliber projectile presenting different aspects to the radar is marked. A noise figure of 10 dB is assumed for the receiver and the projectile is in irradiated at the maximum gain of 30 dBi (see Figure 4).

grating lobes giving rise to multiple beams. An aperiodic phased array would have better performance over a wider bandwidth [17] but is far more complex to design. Each element radiates 100 mW of power, giving a total radiated power for the array of 100 W. The radiation pattern of the main beam for this array of antenna is shown in Figure 4. The beam can be electronically scanned give a spatial sweep and the location of the projectile found to an accuracy of $\sim$ 0.1 degree (see Figure 4). A 7.62 mm projectile could be detected and identified even when travelling directly along the axis of the radar beam, thus

Table 1. Fundamental CNR from three different caliber rounds; the results obtained by numerical simulation and by experimental measurement in the laboratory are compared. The data was converted to a time domain trace and subject to the GPOF algorithm to decompose into CNR [16].

Projectile Diameter (Caliber)	**Fundamental Resonant Frequency ν_1 Experimental in bold type, simulation in normal**	**Fundamental Resonance Lifetime $-\frac{1}{\alpha_1}$ Experimental in bold type, simulation in normal**
13 mm	2.06 GHz, **2.13 GHz**	0.444 ns, **0.35 ns**
7.62 mm	3.78 GHz, **3.52 GHz**	0.182 ns, **0.149 ns**
5.56 mm	4.61 GHz, **5.01 GHz**	0.143 ns, **0.125 ns**

presenting the lowest possible RCS ($-14.77\,\mathrm{dBcm}^2$), by the phased array described at ranges below 27 metres (see Figure 5). For more favourable aspects the effective range of detection and identification increases up to a maximum of 109 metres when the projectile is orientated at a right angle to the radar beam and the radar beam is polarised such that the electric field is aligned along the length of the projectile. If the projectile is aligned such that the electric field is perpendicular to the length of the projectile then the RCS is smaller and the effective range is reduced to 41 metres. Interference from flying insects is unlikely as insects typically have a smaller RCS [18], $2\times10^{-3}-1\times10^{-1}\,\mathrm{dBcm}^2$, than that of a metallic man made projectile of the calibers discussed and would not posses any well defined CNR.

5. SUMMARY

The detection and identification of in flight projectiles by measurement of their CNR is entirely feasible. The RCS of projectiles in flight is sufficient in magnitude, at the microwave frequencies where these objects have their fundamental resonances, to allow the detection, tracking and identification of such objects at considerable ranges of up to $\sim$ 100 meters, see Figure 5. A possible method of realizing such a system is outlined using a phased array of antenna elements to spatially steer an ultra wide bandwidth radar beam; identification is achieved by transmission of microwave frequencies which encompass the fundamental complex natural resonances of a range of typical caliber projectiles (1.5–5.5 GHz). Analysis of the frequency content

of the scattered radar waveforms provides the signature that enables the caliber of the projectile to be identified. Although the detection of in flight projectiles is not necessarily enhanced over other possible HFI systems the robust identification of projectile calibers provides valuable information which is not available at other radar frequency bands. It is this ability to identify the type of projectile which is novel and distinctive for the discussed application, although the use of CNR to identify objects is very well known [19–22].

REFERENCES

1. Baum, C. E., "On the singularity expansion method for the solution of electromagnetic interaction problems," Interaction Notes, Note 88, Air Force Weapons Laboratory, 1971.
2. Baum, C. E., "The singularity expansion method: Background and developments," *IEEE Antennas and Propagation Society Newsletter*, 1986.
3. Wang, Y. and N. Shuley, "Complex resonant frequencies for the identification of simple objects in free space and lossy environments," *Progress In Electromagnetics Research*, Vol. 27, 1–18, 2000.
4. Lee, J. H. and H. T. Kim, "Radar target discrimination using transient response reconstruction," *Journal of Electromagnetic Waves and Application*, Vol. 19, No. 5, 655–669, 2005.
5. Toribio, R., J. Saillard, and P. Pouliguen, "Identification of radar targets in resonance zone: E-pulse techniques," *Progress In Electromagnetics Research*, Vol. 43, 39–58, 2003.
6. Berni, A. J., "Target identification by natural resonant estimation," *IEEE Trans. Aerospace Electron. Syst.*, Vol. 11, No. 2, 147–154, 1975.
7. Mie, G., "Beitrage zur optik truber medien, speziell kolloider metallosungen," *Annalen der Physik*, Vol. 4, No. 25, 377–445, 1908.
8. Hey, J. S., G. S. Stewart, J. T. Pinson, and P. E. V. Prince, "The scattering of electromagnetic waves by conducting spheres and discs," *Proc. Phys. Soc. B*, Vol. 69, 1038, 1956.
9. Lui, H. and N. V. Shuley, "Radar target identification using a banded E-pulse technique," *IEEE Trans. Antennas Propag.*, Vol. 54, No. 12, 3874–3881, 2006.
10. Harmer, S. W., D. A. Andrews, N. D. Rezgui, and N. J. Bowring, "Detection of handguns by their complex natural resonant

frequencies," *IET Microw. Antennas Propag.*, Vol. 4, No. 9, 1182–1190, Sep. 2010.

11. Chauveau, J., N. de Beaucoudrey, and J. Saillard, "Characterization of perfectly conducting targets in resonance domain with their quality of resonance," *Progress In Electromagnetics Research*, Vol. 74, 69–84, 2007.
12. Kennaugh, E. M. and D. L. Moffatt, "Transient and impulse response approximations," *Proceedings of the IEEE*, Vol. 53, 893–901, Aug. 1965.
13. Chuang, C. W. and D. L. Moffatt, "Natural resonances of radar targets via Prony's method and target discrimination," *IEEE Trans. Aero. and Elect. Sys.*, Vol. 12, No. 5, 583–589, 1976.
14. Baum, C. E., E. J. Rothwell, K. M. Chen, et al., "The singularity expansion method and its application to target identification," *Proc. IEEE*, Vol. 79, No. 10, 1481–1492, 1991.
15. Secmen, M. and G. Turhan-Sayan, "Radar target classification method with reduced aspect dependency and improved noise performance using multiple signal classification algorithm," *IET Radar, Sonar and Navig.*, Vol. 3, No. 6, 583–595, 2009.
16. Hua, Y. and T. K. Sarkar, "Generalized pencil-of-function method for extracting poles of an EM system from its transient response," *IEEE Trans. Antennas Propag.*, Vol. 37, No. 2, 229–234, 1989.
17. Bray, M. G., D. H. Werner, D. W. Boeringer, and D. W. Machuga, "Optimization of thinned aperiodic linear phased arrays using genetic algorithms to reduce grating lobes during scanning," *IEEE Trans. Antennas Propag.*, Vol. 50, No. 12, 1732–1742, Dec. 2002.
18. Richter, J. H. and D. R. Jensen, "Radar cross-section measurements of insects," *Proc. IEEE*, Vol. 6, 143–144, 1973.
19. Wilton, D. R. and K. R. Umashankar, "Parametric study of an L-shaped wire using thesingularity expansion method," Interaction Notes, Note 152, Air Force Weapons Laboratory, 1973.
20. Baum, C. E., "Concerning the identification of buried dielectric targets," Interaction Notes, Note 504, Philips Laboratory, Jul. 24, 1994.
21. Baum, C. E., "Combining polarimetry with SEM in radar backscattering for target identification," Interaction Notes, Note 585, Air Force Weapons Laboratory, May 23, 2003.
22. Baum, C. E., et al., "The singularity expansion method and its application to target identification," *Proc. IEEE*, 1481–1492, 1991.